MINISTRY OF EDUCATION AND SCIENTIFIC RESEARCH
National University of Science and Technology POLITEHNICA Bucharest
Faculty of Industrial Engineering and Robotics

Iulian-Constantin COROPEȚCHI

DOCTORAL THESIS

-SUMMARY-

Artificial intelligence-based optimization for the design of special configuration topological structures

Scientific coordinator,

***Professor* Dan Mihai CONSTANTINESCU**

- 2025 -

THE COMMITTEE FOR THE DOCTORAL THESIS

President	Professor, PhD Diana POPESCU	National University of Science and Technology POLITEHNICA Bucharest
Scientific coordinator	Professor, PhD Dan-Mihai CONSTANTINESCU	
Referent	Academician, PhD Dorel BANABIC	Technical University of Cluj-Napoca
Referent	Professor, PhD Adrian-Marius PASCU	„Lucian Blaga” University of Sibiu
Referent	Associate professor, PhD Florin BACIU	National University of Science and Technology POLITEHNICA Bucharest

CONTENTS

INTRODUCTION

Motivation for choosing the research topic

The study of optimization processes in structural design is increasingly necessary due to the high demand for lightweight, efficient and multifunctional materials and structures. Traditional design-by-trial or purely analytical approaches are often limited in capturing the full potential of complex structures, especially when working with non-intuitive geometries such as auxetic materials or deformable mechanisms. Optimization provides a systematic way to explore vast design spaces, identify innovative solutions and balance competing objectives such as stiffness, strength, weight reduction or deformation characteristics. In the context of modern engineering challenges, where material efficiency and performance must go hand in hand with sustainability and cost-effectiveness, optimization is no longer a luxury but a necessity.

At the same time, the motivation to study optimization processes also comes from the advances in additive manufacturing and artificial intelligence-based methods. New manufacturing technologies enable the realization of complex geometries and multi-material architectures that were previously impossible to produce, while machine learning methods provide powerful tools to manage the complexity of such problems. By integrating optimization frameworks with experimental validation, researchers can bridge the gap between theoretical models and practical applications, ensuring that proposed solutions are both feasible and effective. Ultimately, the motivation to study this optimization process lies in its potential to enable the design of next-generation mechanical metamaterials and structures with customized properties, opening up new possibilities in aerospace, automotive, biomedical devices, and beyond.

Relevance and importance of the doctoral research

The relevance of this research lies in the fact that traditional design methodologies are often insufficient to handle highly complex, non-intuitive structures such as cellular structures [1], spinoidal structures [2], or deformable mechanisms [3]. These specially configured structures cannot always be designed using conventional methods, making optimization tools indispensable for identifying effective solutions. By systematically formulating the problem and applying advanced optimization techniques, this research contributes to a deeper understanding of how to design structures with customized properties that would otherwise remain unexplored.

Another important aspect is that structural optimization addresses a common problem: balancing conflicting objectives, such as minimizing weight, maximizing stiffness, or allowing large deformations without compromising strength. In many fields, even small improvements in material efficiency or mechanical performance translate into significant technological and economic benefits. Therefore, this research offers both theoretical contributions to the field of optimization and practical relevance in solving real-world design problems.

The link with additive manufacturing (AM) further reinforces the importance of research. AM technologies enable the manufacture of highly complex structures that were previously impossible to produce using traditional manufacturing methods. This link between optimization and AM ensures that theoretical designs can be physically realized. Furthermore, the research addresses manufacturing constraints, ensuring that optimized solutions are not only theoretically optimal but also feasible in production environments.

A key contribution of this work is the integration of multiple materials into the optimization framework. Unlike single-material structures, multi-material configurations offer a richer design space. For example, combining rigid and flexible materials in an optimized structure can produce auxetic behavior. This makes the research particularly relevant for the development of mechanical metamaterials, which have applications ranging from impact energy absorption to medical implant design

Equally important is the experimental validation of optimized structures. Although simulations can provide valuable information, they are often limited by simplifying assumptions. By testing base materials and optimized structures under laboratory conditions, this research ensures that the predicted properties are achievable in practice. The use of advanced experimental tools, such as digital image correlation (DIC), further enhances the reliability of the results and strengthens confidence in the optimization framework.

Ultimately, the research contributes to the long-term development of strategies for designing special structures. By combining optimization algorithms, machine learning approaches, and experimental validation, it establishes a framework that can evolve as new technologies and computational tools emerge. This perspective ensures that the relevance of the research extends beyond its immediate results, serving as a foundation for future studies in structural optimization and metamaterial design.

Purpose and objectives of the doctoral research

The main goal of this work is to develop an optimization methodology based on artificial intelligence that can be easily adapted to various problems in order to determine new geometric configurations of special configuration structures.

In order to achieve the proposed goal, the following main objectives are pursued:

1. Analysis of the literature on special topological structures such as truss structures, lattice, cellular microstructures, spinoidal structures, and deformable mechanisms, as well as additive manufacturing technologies that enable the creation of these special structures and compatible materials.
2. Study of the types of algorithms used in structural optimization in three broad categories: gradient-based algorithms, direct search algorithms, and artificial intelligence algorithms.
3. Conducting a comparative study on the performance of direct search algorithms in solving an optimization problem for a repetitive composite structure.
4. Studying and implementing artificial intelligence methods that can be used to predict the mechanical properties of structures or to discover new types of configurations according to defined needs.
5. Manufacturing optimized structures using additive manufacturing technologies.
6. Experimental testing of structures manufactured using various standardized methods in order to validate the optimization process.

Structure of the doctoral thesis

The doctoral thesis is structured in seven chapters, plus bibliographical references.

Chapter 1 presents a review of the literature on special configuration structures such as lattice, cellular structures, spinoidal structures, and deformable mechanisms. The latest research on the design methods, numerical and experimental verification of these structures is studied. The second part of the chapter analyzes the seven additive manufacturing technologies that can be used to create special configuration structures.

Chapter 2 provides an analysis of existing types of structural optimization and methods for adjusting optimization processes. The main algorithms for solving optimization problems are studied, divided into gradient-based algorithms, direct search algorithms, and artificial intelligence algorithms.

Chapter 3 provides a comparative analysis of direct search methods for solving an optimization problem of a repetitive composite structure in order to determine the solution with maximized Young modulus along the two orthogonal directions. The implementation of the algorithms in the Python programming language is described, and the entire workflow with the PyAnsys package is presented, which allows the integrated use of the finite element analysis program directly in the mathematical formulation of the algorithms. The four optimization algorithms studied, greedy, SA (Simulated Annealing), GA (Genetic Algorithm), and PSO (Particle Swarm Optimization), are evaluated according to different metrics based on the computational effort required and the quality of the solution provided.

Chapter 4 presents two artificial intelligence methods that can be used to solve structural optimization problems: a convolutional neural network (CNN) and a variational autoencoder (VAE). The methods of constructing networks are analyzed, as well as the main parameters underlying them and how they are trained and validated. The convolutional network is trained to predict the mechanical properties of structures, and the generative abilities of the variational autoencoder are exploited.

Experimental research on a case study is carried out in Chapter 5. Structures optimized by the algorithms developed in the previous chapters are produced using additive manufacturing technologies, after which various tests are performed to determine the mechanical properties of the materials used. The experimental results are compared with the numerical results to validate the optimization process.

Chapter 6 presents a synthesized and structured approach to using the developed optimization methodology. The main steps that the user must follow are presented, from defining the optimization problem to choosing algorithms, training, and numerical and experimental validation of solutions.

Chapter 7 presents the general conclusions, personal contributions, and future research directions.

CHAPTER 1 – CURRENT STATUS OF THE DESIGN OF TOPOLOGICAL STRUCTURES WITH SPECIAL CONFIGURATIONS

Unlike classical structures, which are typically designed with homogeneous materials and conventional geometries to carry loads and perform basic mechanical functions, specially configured topological structures such as lattice, cellular microstructures, spinoidal structures, deformable mechanisms, and others, exploit micro- or meso-level geometry to achieve unique and often counterintuitive properties. These engineered materials or structures can exhibit negative Poisson's ratios, programmable stiffness, deformable geometries, enhanced energy absorption capabilities, and other mechanical properties. Their properties arise not only from the properties of the base materials, but also from their geometric configuration, allowing users to fabricate such structures to exhibit application-specific responses.

Truss structures are composed of straight elements connected at nodes, forming triangular units that efficiently carry loads through axial forces. Traditionally used in bridges, towers, and structures, trusses offer high strength-to-weight ratios. In advanced applications, truss-like architectures are miniaturized into lattice materials, where their geometry can be optimized to achieve specific properties of stiffness, strength, or energy absorption [4]. An example of an optimized truss structure is shown in Fig. 1 (a)

Cellular structures consist of repetitive cells, often in foam-like arrangements, with open or closed cells. These architectures can significantly reduce weight while maintaining structural integrity, making them ideal for lightweight components. The geometry of the cells—hexagonal, octet, or random—can be optimized to influence thermal, acoustic, and mechanical performance. Cellular structures are widely used in packaging, aerospace panels, and energy absorption layers [5], [6]. An example of a cellular structure is shown in Fig. 1 (b).

Spinodal structures are continuous geometries inspired by phase separation phenomena in metallurgical processes. They feature smooth, interconnected areas and are often generated computationally using spinodal decomposition simulations. These structures offer high surface-to-volume ratios, making them suitable for filtration, biomedical implants, and multifunctional materials that require coupled properties such as stiffness and permeability [7]. An example of a spinodal structure is shown in Fig. 1 (c).

Compliant mechanisms achieve movement through elastic deformation of their structure, rather than using discrete joints or hinges. This allows for simpler monolithic geometries with fewer parts and reduced maintenance. These mechanisms are widely used in precision engineering, biomedical devices, and soft robotics. Their performance is highly sensitive to geometry and material selection, making computational optimization essential for their design [3]. An example of a plane compliant mechanism obtained through optimization is shown in Fig. 1 (d).

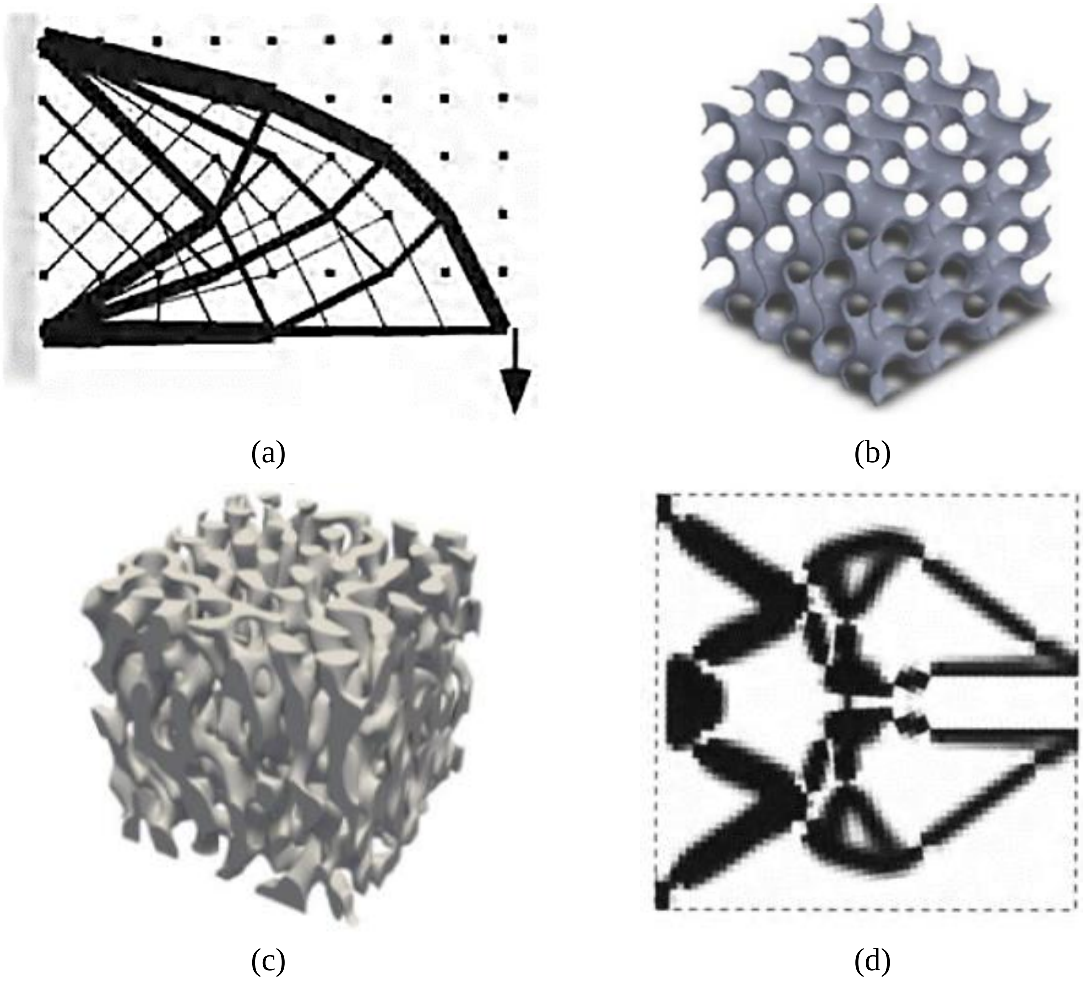

Fig. 1-1 Examples of optimized structures: (a) truss structure [8]; (b) TPMS cellular structure [9]; (c) spinoidal structure optimized to mimic bone structure [7]; (d) gripper compliant mechanisms obtained through optimization [8]

Equally important to this evolution has been the development of manufacturing technologies, particularly additive manufacturing. Many of these architectured structures feature complex, highly detailed geometries that are impractical or impossible to manufacture using traditional methods. Additive manufacturing allows for the layer-by-layer construction of complex internal shapes, with a high degree of freedom in both geometry and material composition. Techniques such as material extrusion, photopolymerization, or powder bed fusion have paved the way for the physical realization of computationally designed structures at multiple scales—from macro-engineered lattices to cellular or spinodal patterns at the micro scale. This synergy between design and manufacturing has not only enabled the production of previously theoretical structures, but has also accelerated innovation in fields such as biomechanics, aerospace, and defense.

In this chapter, we explored the emerging field of specially configured topological structures, focusing on their geometry, function, fabrication, and testing. These advanced structures offer unique mechanical behavior that is difficult to achieve with classical structures. Their custom topologies enable improved performance, such as high strength-to-weight ratios, auxetic behavior, controlled deformation, or energy absorption, making them vital in aerospace, biomedical devices, and lightweight structural systems.

The evolution of these structures has been closely linked to advances in additive manufacturing (AM). The seven standard AM processes defined by ISO/ASTM 52900:2021 [10]—material extrusion, photopolymerization, powder bed fusion, material jetting, binder jetting, direct energy deposition, and sheet lamination—have each opened up specific opportunities for the manufacture of complex, functional, or multi-material structures. These technologies circumvent traditional geometric constraints, enabling the production of highly complex shapes required by modern engineered materials.

Equally important is the role of material selection in AM. Polymers, metals, and ceramics are now commonly adapted to different AM processes, each offering specific mechanical, thermal, or chemical advantages. For example, thermoplastics such as PLA and TPU are widely used in extrusion-based AM, while metals such as Ti-6Al-4V are crucial for powder bed fusion and direct energy deposition. Ceramic-based AM, although more difficult, is gaining ground in the medical field and applications involving high temperatures. The combination of structural design and material properties is essential for tuning the performance of specially configured structures.

Finally, the chapter reviewed the experimental testing methodologies required to validate and characterize these structures. Techniques range from classical mechanical testing (tensile, compression, and bending tests) to advanced digital image correlation (DIC) and fatigue or cyclic loading analysis. These methods ensure that new topologies not only meet theoretical expectations but also function reliably under practical loading conditions.

In conclusion, the convergence of structural design, advanced materials, state-of-the-art additive manufacturing processes, and robust experimental testing has created a new design paradigm. These specially configured structures offer promising solutions to future engineering challenges, especially when optimized through computational methods and validated through experimental research. Continued development in this area will likely lead to even more adaptive, multifunctional, and intelligent material systems tailored for real-world applications.

CHAPTER 2 – STRUCTURAL OPTIMIZATION PROCESSES AND ALGORITHMS ANALYSIS

Structural optimization has been used in mechanical engineering for many years, for example to minimize the mass of material used and the total deformation energy of structures while maintaining their mechanical strength [8]. This includes dimensional optimization, shape optimization, and topological optimization, and leads to the generation of more complex geometries for structures used in the field, geometries that cannot always be achieved with conventional manufacturing processes.

Structural optimization aims to increase the (user-defined) performance of a mechanical structure using a mathematical formulation. This can be dimensional optimization, shape optimization, or topological optimization. Structural optimization can refer to classical topological optimization, composite optimization, deformable mechanism optimization, cellular microstructure optimization, or combinations of these.

According to [11], any structural design process comprises three stages. The first stage is conceptual, in which the structural system and its rough form are chosen. This stage draws on the designer's experience and judgment in a qualitative manner and has no algorithmic basis, making it very difficult to automate. The second stage, preliminary design, involves establishing the defining shape and geometry. The final stage, detailed design, involves local and detailed modification of the structure's geometry. Structural optimization processes can be applied starting with the second stage or, in some cases, in the third stage.

A constrained optimization problem is written mathematically in the following form:

$$\begin{aligned} &\min_{x\in\mathbb{R}^n} f(x) \\ &\text{subject to: } Cx \le d,\ g(x)\le 0,\ l\le x\le u,\ Ax=b,\ h(x)=0 \end{aligned} \tag{2-1}$$

where $l,u\in\mathbb{R}^n$, $d\in\mathbb{R}^{m1}$, $b\in\mathbb{R}^{p1}$, $C\in\mathbb{R}^{m1\times n}$, $A\in\mathbb{R}^{p1\times n}$, and $g(x):\mathbb{R}^n\to\mathbb{R}^{m2}$, $h(x):\mathbb{R}^n\to\mathbb{R}^{p2}$ are multidimensional functions (vectors), representing nonlinear inequality and equality constraints, respectively, and x represents the optimization variable.

This chapter explored fundamental and advanced approaches to structural optimization, with a particular focus on the three classical methods—dimensional optimization, shape optimization, and topology optimization—and their computational strategies. Each of these levels of optimization plays a distinct role in the design process. Dimensional optimization, as a basic approach, deals with adjusting the dimensions or thicknesses of cross-sections within predefined layouts to achieve efficiency and weight reduction. Shape optimization advances this by refining the external boundaries of structures, improving performance without altering their topology. Finally, topological optimization represents the most general and powerful strategy, allowing the discovery of completely new material patterns and structural shapes that are often counterintuitive and impossible to achieve through traditional design approaches.

An important method in topology optimization is the SIMP technique. This approach has proven extremely effective in reducing the discrepancy between continuous optimization formulations and discrete models. However, SIMP and related density-based methods are not without challenges. Numerical instabilities, such as chessboard patterns, dependence on mesh size, and the occurrence of non-physical solutions, often complicate the optimization process. To address these issues, filtering techniques and regularization strategies have been implemented, while interface evolution modeling has emerged as a promising alternative, providing a consistent mathematical framework for controlling structural boundaries and ensuring smooth transitions between material phases. Together, these developments highlight the importance of not only formulating optimization problems, but also ensuring their robustness, reliability, and applicability in practical engineering contexts. The influence of implementing regularization techniques on the optimal solution can be seen in Fig. 2 1.

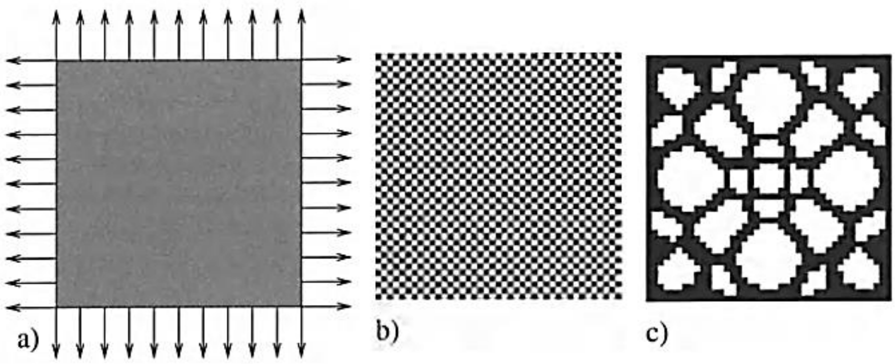

Fig. 2-1 The chessboard problem demonstrated on a rectangular structure subjected to biaxial loading and modeled with Q4 elements. a) problem model, b) solution obtained without applying constraints to remove the chessboard, c) solution obtained with constraints applied [8]

Beyond problem formulation, a crucial aspect of structural optimization lies in the algorithms used to solve the problem. This chapter has reviewed three major categories: gradient-based methods, direct search methods, and artificial intelligence-based approaches. Gradient-based techniques remain the most widely used in structural optimization due to their efficiency and solid mathematical foundation, especially for problems where derivative information is available and accurate. However, their dependence on differentiable objective functions limits their applicability to highly nonlinear or discrete optimization problems.

In contrast, direct search methods—such as the greedy algorithm, genetic algorithms, or particle swarm optimization—do not require derivative information, making them attractive for nonlinear problems where the objective function is not differentiable or for results obtained through experimental methods. Their robustness is often offset by computational cost, especially in high-dimensional search spaces, but they remain an important tool in applications where gradients are either unavailable or unreliable.

Finally, the rise of artificial intelligence has opened up new frontiers in structural optimization. Methods based on neural networks have demonstrated the ability to explore vast and complex design spaces, capture nonlinear behaviors, and integrate seamlessly with simulation data. AI-based methods also offer potential in data-driven optimization, where machine learning models approximate performance, drastically reducing computational cost. However, challenges remain in terms of convergence reliability, interpretability, and integration with physics-based constraints. Combining artificial intelligence with traditional optimization frameworks, particularly hybrid approaches, is a promising direction for future research.

Taken together, the discussion of methods, numerical instabilities, and computational algorithms illustrates the interconnected nature of structural optimization. Their successful application is not just a matter of choosing an algorithm, but rather of balancing mathematical rigor, computational efficiency, and physical viability. The ongoing development of filtering and regularization methods, combined with advances in artificial intelligence-based optimization, suggests that the future of structural optimization will increasingly involve hybrid strategies—integrating gradient-based rigor, direct search robustness, and machine learning adaptability.

From a broader perspective, structural optimization is more than a computational exercise; it is a design philosophy that is reshaping modern engineering. The ability to systematically identify optimal configurations allows engineers to reduce material consumption and discover new structural concepts. These advances have a particular impact when combined with modern manufacturing methods, such as additive manufacturing, which can bring optimized topologies into physical reality without the limitations of traditional manufacturing. As such, structural optimization is not only a powerful theoretical tool, but also a practical enabler of innovation in aerospace, automotive, biomedical, civil engineering, and other fields.

In conclusion, the evolution of structural optimization has progressed from classical dimensional adjustments to advanced topology design, supported by sophisticated algorithms and numerical models. Challenges such as the use of chessboard configurations, dependence on discretization fineness, and solution instability have stimulated the development of filters and formulations for modeling interface evolution, strengthening the reliability of the optimization process. Meanwhile, the expansion of available computational techniques has enriched the toolkit available to both researchers and engineers involved in manufacturing. Looking ahead, the integration of these diverse methods, together with high-fidelity simulations and advanced manufacturing technologies, will continue to push the boundaries of structural design, leading to truly optimized, multifunctional, and adaptive structures capable of addressing the engineering challenges of the future.

CHAPTER 3 – COMPARATIVE ANALYSIS OF DIRECT SEARCH METHODS FOR SOLVING STRUCTURAL OPTIMIZATION PROBLEMS

This chapter focuses on the analysis of direct search methods applied to structural optimization problems. These approaches are valued for their simplicity, versatility, and broad applicability, especially in cases where gradient information is unavailable or unreliable. Unlike gradient-based methods, direct search techniques do not require explicit derivatives of the objective function. Instead, they systematically explore the design space through sequences of sampled solutions, which makes them particularly suitable for problems with non-differentiable, discontinuous, or computationally expensive objective functions.

The purpose of this chapter is to evaluate and compare different direct search algorithms in terms of their effectiveness in solving structural optimization problems. For each method, the discussion highlights the main advantages, limitations, and practical considerations to better understand the contexts in which each approach is most effective. The direct search methods examined include: brute force, greedy algorithms, simulated annealing (SA) algorithms, genetic algorithms (GA), and particle swarm optimization (PSO).

In order to compare and evaluate direct search methods, a composite material optimization problem is defined. The chosen problem is inspired from [12] with some changes. First, a two-dimensional periodic domain (Fig. 3-1 (a)) consisting of two different materials was considered, for which the elastic moduli E_1 and E_2 and the Poisson coefficients ν_1 and ν_2 are known. In the given domain, the proportions of the two materials are equal. The objective proposed for this optimization problem is to determine the optimal distribution of the two materials in the given domain that ensures maximum and equal effective properties of the elastic moduli in the two orthogonal directions of the domain.

Analyzing the given domain, a representative cell is identified according to the one shown in Fig. 3-1 (b) which, for symmetry reasons, can only be analyzed on a quarter of a cell – Fig. 3-1 (c). This quarter cell, with overall dimensions a x b, for the present problem $a = b = 1$ mm, can be analyzed using appropriate boundary conditions (Fig. 3-1 (d)) and a mesh with only 16 equal quadrilateral finite elements. To simulate the behavior of this quarter cell in the periodic domain, the symmetry condition in displacements along the Ox axis on the x=0 side is applied, respectively the symmetry condition in displacements along the Oy axis on the y=0 side. At the same time, coupling in displacements along the Ox axis on the x=a side and coupling in displacements along the Oy axis on the y=b side are applied. These boundary conditions imposed on the representative quarter cell are equivalent to performing the calculation over the entire periodic domain.

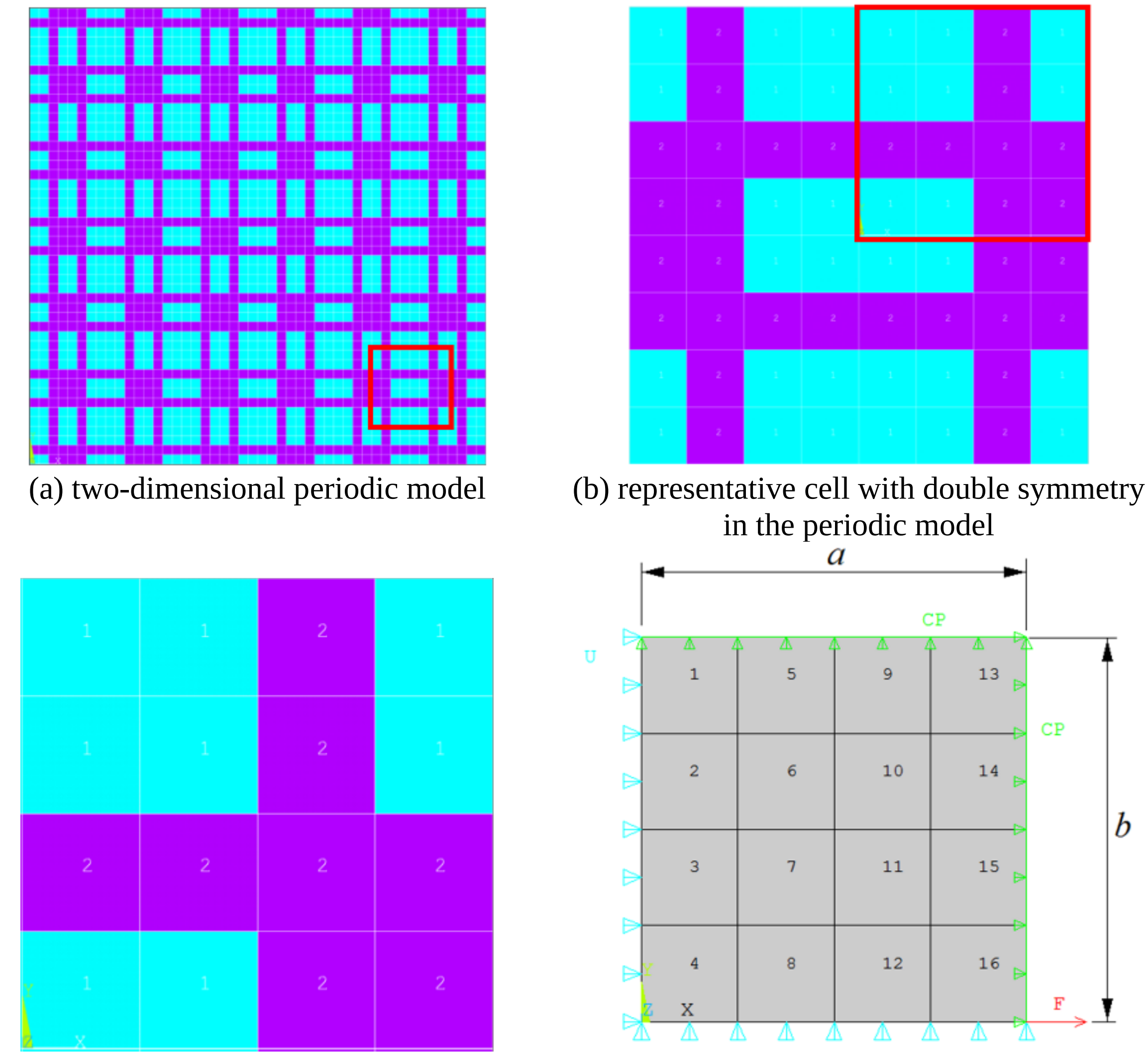

(a) two-dimensional periodic model

(b) representative cell with double symmetry in the periodic model

(c) one quarter of the representative cell used in the analysis

(d) numbering of finite elements and boundary conditions imposed

Fig. 3-1 Description of the two-dimensional periodic domain consisting of two materials with different properties that appear in equal proportions in the domain

For the present problem, a parameter of interest for the representative cell is the effective elastic modulus, which can be defined by the relation (3-1)

$$E_{eff} = \frac{\bar{\sigma}}{\bar{\varepsilon}} = \frac{\frac{1}{V}\sum_{i=1}^{NE} V_i \sigma_i}{\frac{1}{V}\sum_{i=1}^{NE} V_i \varepsilon_i} \tag{3-1}$$

where:

- E_{eff} is the effective elastic modulus;
- $\bar{\sigma}$ is the averaged stress over the entire domain;
- $\bar{\varepsilon}$ is the averaged strain over the entire domain;
- V is the volume of the entire domain;
- NE is the number of elements in the domain;

– V_i is the volume of element *i*;
– σ_i is the average stress in element *i* (component in X or Y direction);
– ε_i is the average strain in element *i* (component in X or Y direction).

A convergence study was conducted, from which we can observe that for a solution that has many connected elements in a chessboard pattern, the mesh size plays a very important role. As the number of elements used to mesh a material domain increases, the value of the elastic modulus decreases, but the behavior of the solution when rotating the axes also changes drastically. The most pronounced change can be seen in Poisson's ratio, when the figure becomes antisymmetric as the number of elements in the mesh of a domain increases. In this sense, a mesh with 9 finite elements was applied in each material domain.

Analyzing the solution space presented in Fig. 3-2, the four solutions presented on the right side of the figure are considered to be the optimal solutions for evaluating the performance of the algorithms. The first two solutions have the same objective function value equal to 4.065855 and represent the same solution rotated by 90°. Although this solution does not have equal elastic modules in both directions, the relative error between them is less than 0.2% and is considered optimal. The next two solutions have objective function values equal to 4.027104 and 4.022015, respectively, and have a relative error compared to the first solution of less than 1.1%.

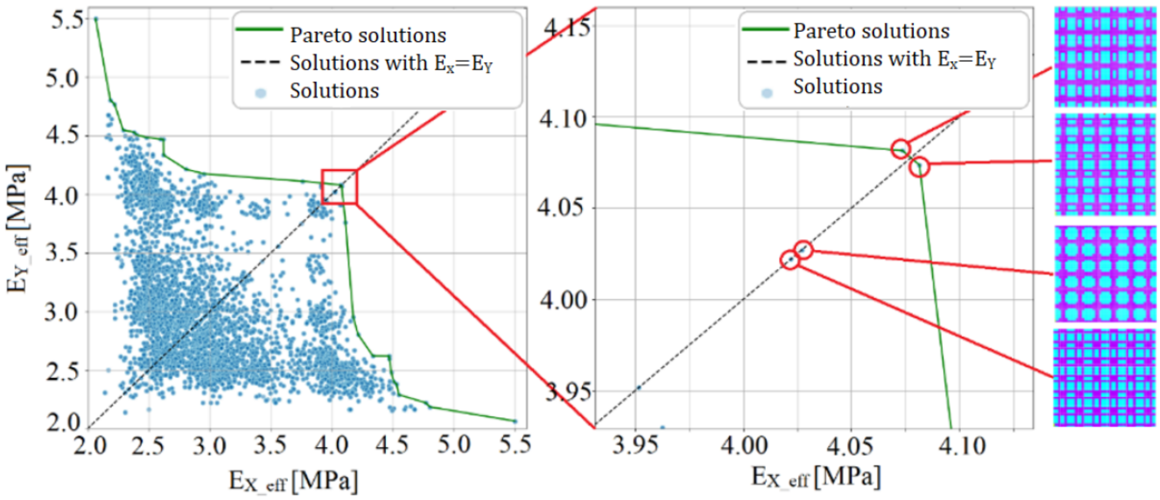

Fig. 3-2 Distribution of all solutions meshed with 9 finite elements per domain and the four solutions considered optimal for evaluating the performance of direct search algorithms

The way in which the algorithms converge over time can be clearly seen in Fig. 3-3, which shows the probability density function (PDF) of the computation time. Since the actual computation time, measured in seconds, is influenced by the performance of the computing system used, it is expressed here by the number of evaluations of the objective function. The statistical analysis in Fig. 3-3 illustrates both qualitatively and quantitatively the performance of the algorithms, with 100 runs for the 4x4 problem for each of them.

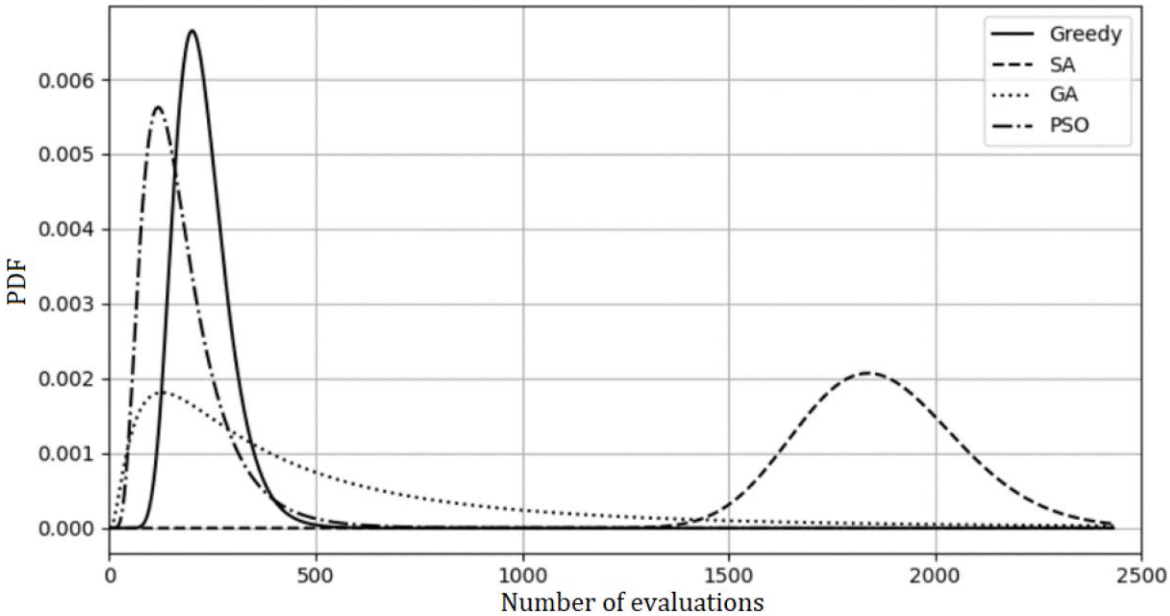

Fig. 3-3 Probability density function for the number of evaluations of the 4 algorithms for the 4x4 problem

Analyzing Fig. 3-3, we can say that for the 4x4 problem, the PSO algorithm presents the best PDF shape with clear symmetry and a pronounced degree of "peaking," which indicates high probabilities that the algorithm will determine the global optimum around the average value of the number of evaluations of the objective function. Similarly, we can draw the same conclusion about the greedy algorithm, which ranks second in terms of PDF shape. As for GA, it can be seen that the PDF shape shows pronounced asymmetry and a low degree of "peaking," indicating a lower probability that a genetic algorithm will reach the global optimum with a number of objective function evaluations close to the average. The probability density for GA is much more scattered than that of the two algorithms analyzed previously. For SA, it can be seen that it shows clear symmetry, but the degree of flattening is similar to GA. The probability that the algorithm will find the global optimum for a number of objective function evaluations around the mean is similar to the probability of the GA algorithm but higher around the mean value.

Regarding the 6x6 problem, since the large number of solutions makes it impossible to perform brute force and determine the global optimum, five runs were performed with the greedy, GA, and PSO algorithms. The reason why SA was not implemented for the 6x6 problem is that its structure is similar to that of the greedy algorithm, practically a chain of greedy algorithms.

In order to make a direct comparison between algorithms, it is necessary to present the evolution of the objective function in relation to the number of evaluations of the function, as each algorithm evaluates a different number of solutions at each iteration. For the 6x6 problem, the greedy algorithm evaluates 324 solutions per iteration, GA evaluates 180 solutions per iteration, and PSO evaluates 30 solutions per iteration. The evolution of the objective function for the first 10,000 evaluated solutions is shown in Fig. 3-4.

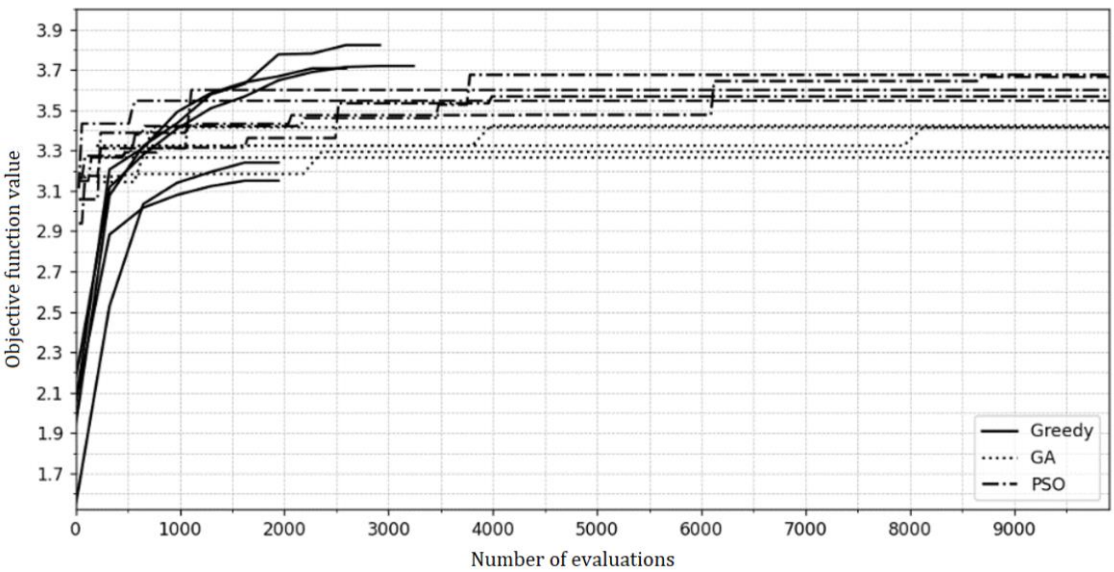

Fig. 3-4 Evolution of the objective function depending on the number of evaluations required for the three algorithms – Greedy, GA, and PSO – the first 10,000 solutions evaluated

We can see in Fig. 3-4 that for the first 1,000 evaluations of the objective function, the three algorithms have comparable results in terms of the value of the objective function. The greedy algorithm is the only one that improves the objective function at each iteration and the one that achieves the highest value of the function equal to 3.822149. At the same time, out of the 5 runs, 2 reach solutions with the weakest results among the three algorithms. It can be seen that the runs for GA and PSO reach around the same value, with an improved value for PSO and fewer evaluations of the objective function.

Since the greedy and PSO algorithms performed best, a hybrid PSO+greedy approach was implemented. Fig. 3-5 shows the average value of the objective function as a function of the average number of evaluations required to achieve that value for the 5 runs for each of the four algorithms presented. The graph shows the computational effort and performance achieved, from which we can conclude that the greedy algorithm has the lowest computational effort but a lower average value of the objective function. The hybrid algorithm has the best average value of the objective function, but the computational effort is higher. At the same time, GA ranks last in terms of the objective function value and the computational effort required.

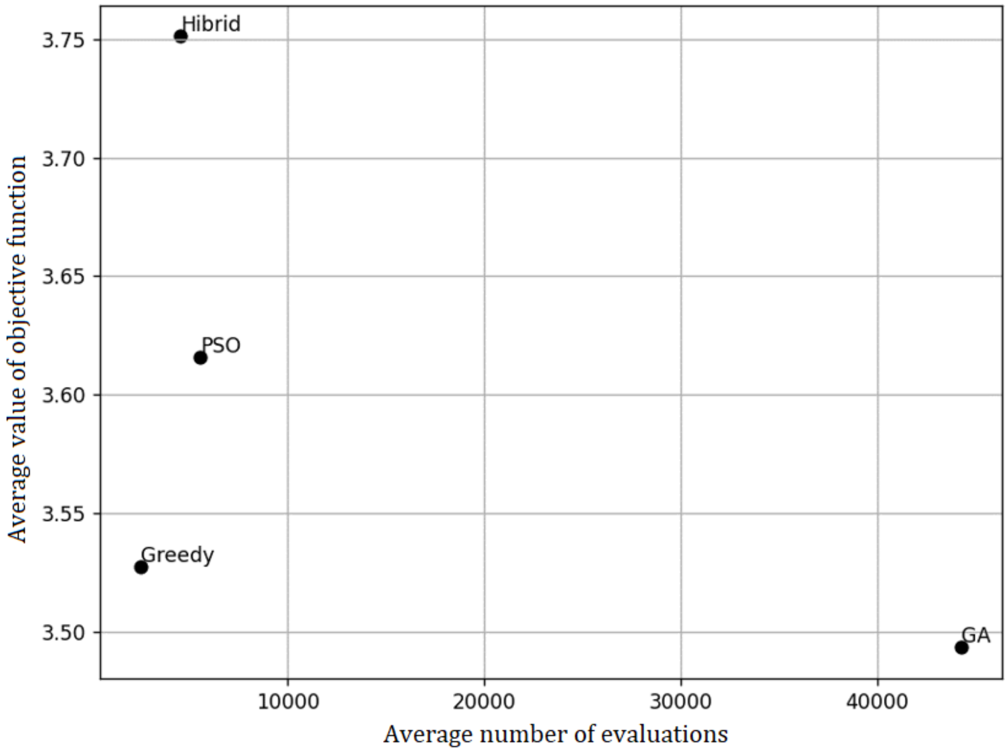

Fig. 3-5 Average value of the objective function depending on the average number of evaluations

This comparative study provides valuable insights into the performance of four optimization algorithms—greedy, SA, GA, and PSO—as well as a hybrid PSO-greedy approach. The algorithms were evaluated based on various metrics, such as convergence speed, solution quality, computational efficiency, and robustness.

The analysis shows that each algorithm has distinct strengths and weaknesses, depending on the characteristics and requirements of the optimization problem. The greedy algorithm, although simple, demonstrates competitive performance in terms of convergence speed, but may suffer from suboptimal solutions. For the small 4x4 problem, all algorithms reach the known global maximum, but the computational effort is different. For the larger 6x6 problem, in the absence of global maximum information, we can see that GA is much more susceptible to local minima blockages than the other algorithms.

The PSO-greedy hybrid approach, which combines the strengths of both algorithms, shows promising results in terms of balancing exploration and exploitation, leading to improved solution quality and convergence speed compared to individual algorithms. In general, choosing the most suitable optimization algorithm depends on various factors, such as problem complexity, computational resources, and optimization objectives.

Research on the comparison of direct search algorithms was published in [13], and the same methods were tested for the optimization of auxetic configurations for other types of geometric configurations [14].

CHAPTER 4 – MACHINE LEARNING METHODS FOR STRUCTURAL OPTIMIZATION

This chapter analyzes machine learning (ML) methods for solving structural optimization problems, methods that offer flexibility, adaptability, and efficiency for a wide range of problems. Unlike traditional gradient-based methods, ML techniques can learn complex relationships and identify patterns in the analyzed data without requiring explicit knowledge of the objective function gradient. These techniques explore the optimization space through learning algorithms, which continuously improve estimates based on feedback, making them suitable for problems with very large search spaces.

The problem chosen for testing ML methods is similar to the problem described in Chapter 3 with a few differences. The same two-dimensional periodic domain is considered, consisting of two different materials with the same values for Poisson's ratios ν_1=0.4 and ν_2=0.2, but with different values for the elastic moduli of the materials, E_1=1 MPa and E_2=100 MPa. In this domain, there are no restrictions on the proportions of the two materials, so that the search space is as unrestricted as possible. The objective of this optimization problem is to determine the optimal distribution of the two materials in the domain so as to ensure minimum effective values of Poisson's ratios in the two orthogonal directions of the domain.

The boundary conditions imposed for the load cases used are the same as in the previous problem. Taking into account the study on the dependence on the mesh size presented in Chapter 3, it is necessary to eliminate solutions that have elements connected in a chessboard pattern from the search space because it has been shown that these introduce significant errors in the calculations as the degree of mesh increases. Thus, a mesh with a single finite element per material domain was retained, but solutions connected in a chessboard pattern were eliminated. In this case, from the analysis of the solutions obtained by brute force, we can see that we have 23,858 solutions that do not contain elements in a chessboard pattern, representing approximately 36.4% of the total 65,536 solutions. The graphical representation of these solutions can be found in Fig. 4-1.

If we analyze Fig. 4-1, we can see that in the lower left corner, we find solutions with a negative value of Poisson's coefficient in a number of 34 configurations, of which 5 are independent, representing less than 0.15% of the entire solution space. The reason why 34 points are not visible in the figure is due to the overlap of some solutions with others in terms of the value of the two coefficients. The 5 independent solutions in periodic form with a negative value for Poisson's coefficient are shown in Fig. 4-2.

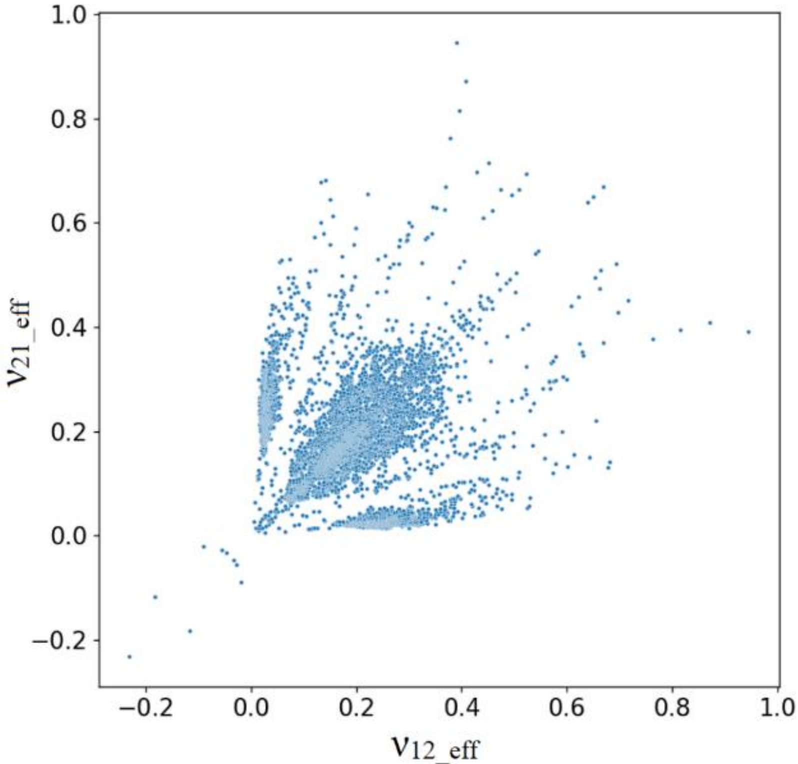

Fig. 4-1 Distribution of all solutions that do not contain elements in a chessboard pattern according to the value of Poisson's coefficients – 4x4 configuration

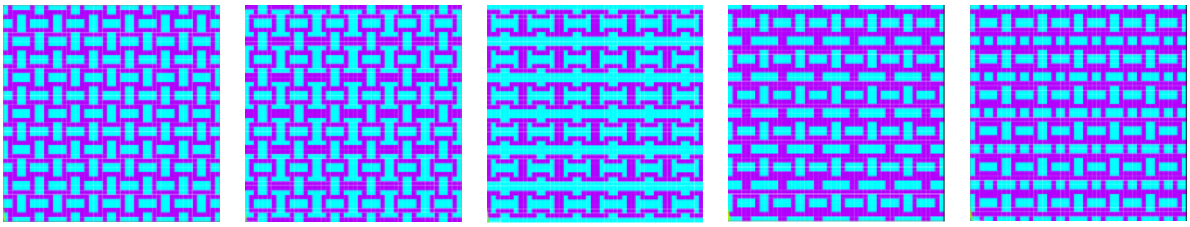

ν_{12} = -0,2307	ν_{12} = -0,1170	ν_{12} = -0,0896	ν_{12} = -0,0553	ν_{12} = -0,0474
ν_{21} = -0,2307	ν_{21} = -0,1827	ν_{21} = -0,0197	ν_{21} = -0,0270	ν_{21} = -0,0327

Fig. 4-2 Periodic representation of solutions with negative Poisson's ratio for the 4x4 model

Two ML models were implemented, a convolutional neural network (CNN) for predicting the Poisson coefficient value based on material distribution and a variational autoencoder (VAE) with the ability to compress the solution space into a latent space and reconstruct the data.

The CNN model proved to be a robust model with a very low prediction error. This implies that the training was performed with a sufficiently large dataset, representing only a fraction of 0.0006% of the entire solution space, and that the parameters in the training process were well set. Finally, we obtain a model that can predict the mechanical properties of a configuration with high accuracy without performing complex calculations similar to finite element analysis. Using this model, we can apply previously studied direct search methods to determine the optimal solution from the solution space.

Previous research has established that the greedy algorithm performs well in solving these problems. In this regard, the algorithm was applied together with the convolutional neural network trained for the 6x6 model. Fig. 4-3 shows the value predicted by the neural network of Poisson's coefficients compared to the actual value verified by finite element analysis for 20 auxetic solutions determined by the algorithm. To increase the performance of the greedy algorithm, at each iteration it checked all configurations obtained by modifying one element in the domain, as well as all configurations obtained by modifying two elements. At each iteration, the algorithm evaluated a maximum of 1,296 solutions, eliminating solutions with elements connected in a chessboard pattern because it was decided a priori to eliminate them due to errors.

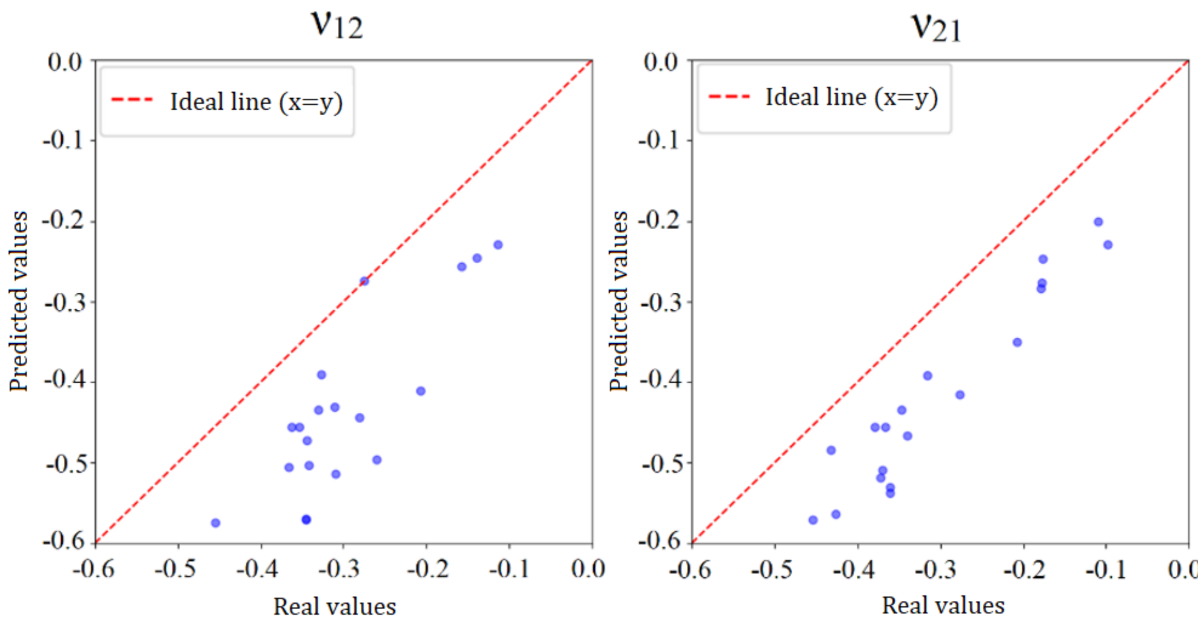

Fig. 4-3 Predicted values versus actual values of Poisson's coefficients for auxetic solutions determined with greedy for the 6x6 model

We can see that the predicted value is much lower than the actual value determined by finite element analysis, with the error reaching up to 133%. This can be explained by the fact that, in the training data set consisting of 280,000 solutions, only about 1,500 solutions are auxetic, approximately 0.53%, presenting negative values for Poisson's ratio with the lowest value encountered equal to -0.371. Thus, although the network has learned to predict the value of Poisson's coefficient for randomly selected solutions, it has a higher error for the extremes of the solution space. At the same time, although the actual value differs greatly from the predicted value, the determined solutions are still auxetic and the order of the predicted coefficients corresponds to the order of the actual coefficients. Fig. 4-4 shows the best 9 solutions determined by the algorithm in the periodic representation of the structure.

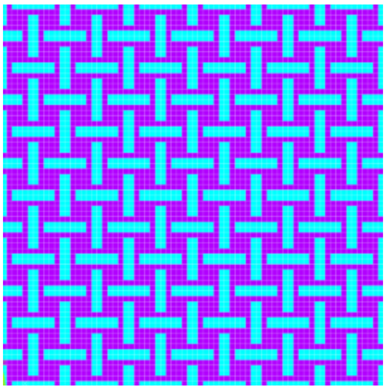

(a) 56,56% hard material

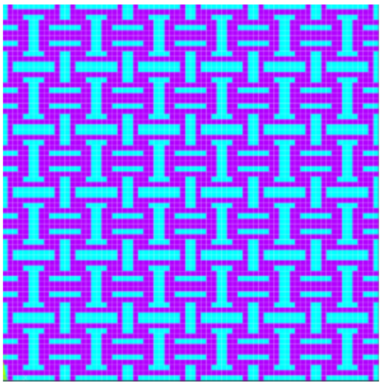

(b) 58,33% hard material

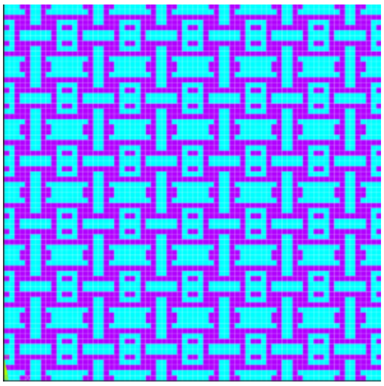

(c) 47,22% hard material

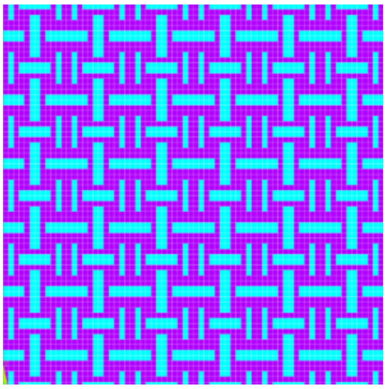

(d) 61,11% hard material

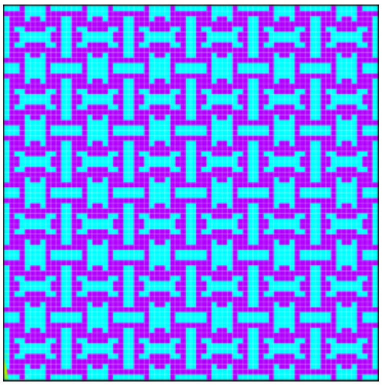

(e) 52,78% hard material

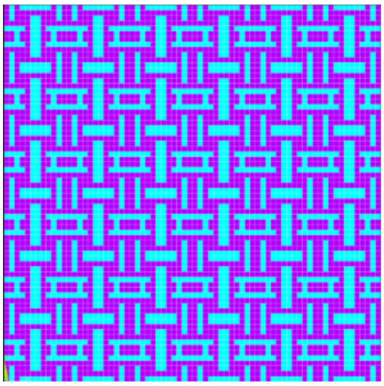

(f) 58,33% hard material

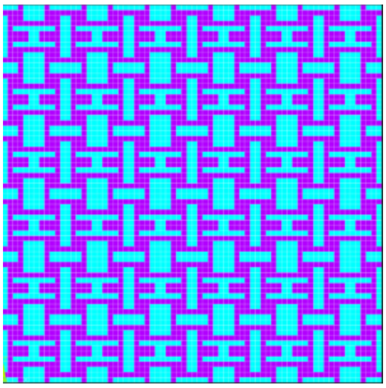

(g) 50,00% hard material

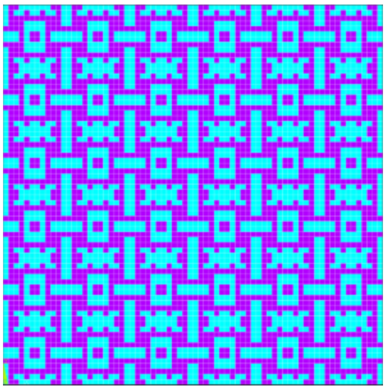

(h) 50,00% hard material

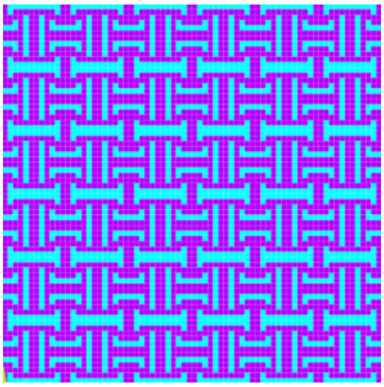

(i) 61,11% hard material

Fig. 4-4 The nine best solutions determined by the greedy algorithm applied together with the convolutional neural network for the 6x6 model

We can see in the figure above that all solutions have a common element, namely the presence of a rectangle of soft material that alternates in orientation along the X (horizontal) or Y (vertical) direction in the periodic structure. The solution with the lowest Poisson's ratio values is the solution in Fig. 4-5 (a) with equal Poisson's ratio values along the two orthogonal directions of -0.4543. Analyzing the literature, we can see that this solution is very similar to the tetra-anti-chiral cell shown in Fig. 4-5 (d). Fig. 4-5 shows the representative cell for the best solution obtained (a), the displacement field for the load case along the X-axis (b) and along the Y-axis (c), as well as the equivalent stresses in the representative cell for the load case along the X-axis (e) and along the Y axis (f). The displacement field and equivalent stresses were obtained by finite element analysis using the load cases presented above, namely traction along the X axis and traction along the Y axis.

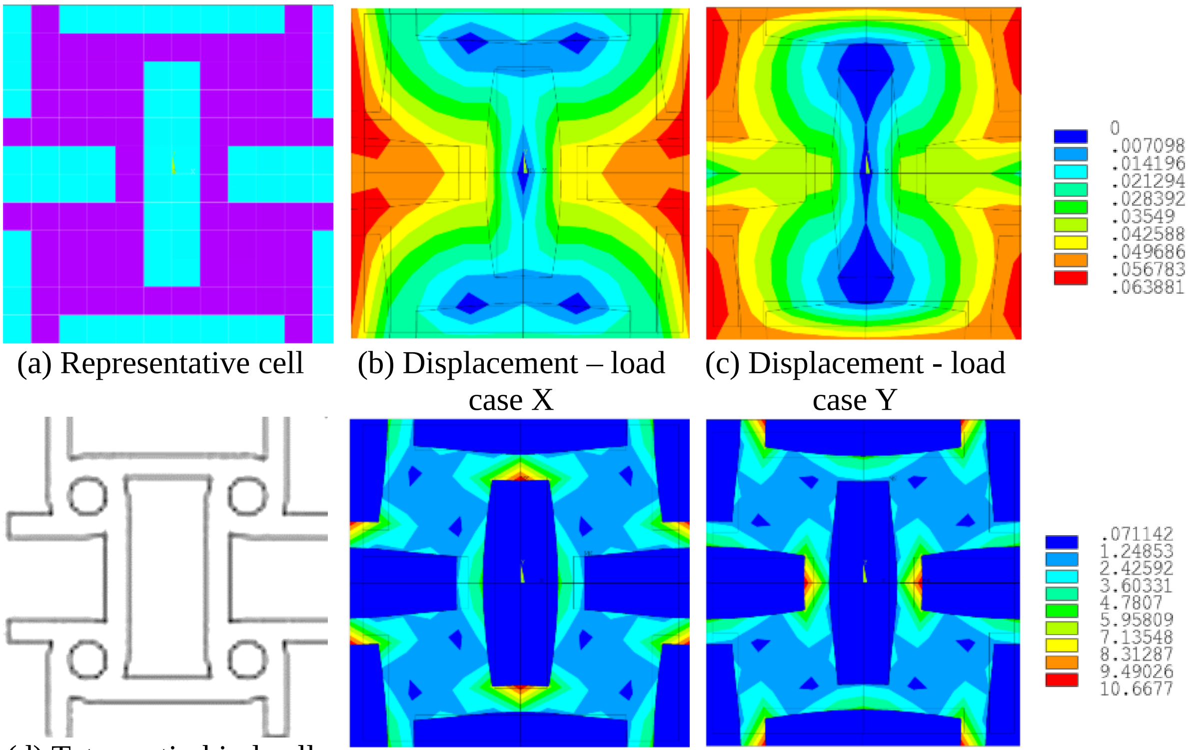

(a) Representative cell (b) Displacement – load case X (c) Displacement - load case Y

(d) Tetra-anti-chiral cell [15] (e) Stress – load case X (f) Stress – load case Y

Fig. 4-5 The solution determined with the lowest Poisson's ratio, the displacement and stress field for the two loading cases, and the similarity to the tetra-anti-chiral cell

Regarding the VAE model, the data presented above suggests that the model has been successfully trained and can compress the input variables into a latent space, after which it can reconstruct the data with high accuracy. The next step in developing this model is to establish a link between the performance of a particular solution, in this case between the values of Poisson's coefficients and the latent space determined by the VAE network. In this case, the size of a problem can be successfully reduced from 36 binary variables representing the configuration of a solution to 12 latent variables sampled from a normal distribution generated by the model's encoder. A well-established correspondence between the value of the objective function and the latent variables facilitates the solution of the optimization problem. In addition to this advantage that the VAE model can offer, it also has generative properties and can generate new structures with superior performance that have not been previously "seen" by the model. An example of the successful application of a VAE model in solving such a problem is presented in [16].

With the VAE model trained on the auxetic solutions dataset, Bayesian optimization was performed in the latent space. The Bayesian optimization process is based on selecting the best locations in the latent space to perform the search using probabilities and a priori information. Unlike stochastic search methods, Bayesian optimization builds a model to predict how promising a particular region is, makes assumptions about similar input data giving similar output data, and the model automatically updates with each point tested. Fig. 4-6 shows the best 5 solutions determined by the Bayesian optimization process in the latent space.

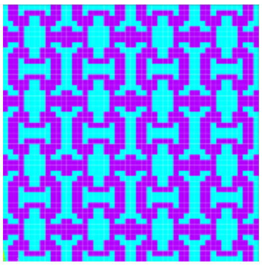

(a) ν_{12} = -0,0995
ν_{21} = -0,2680

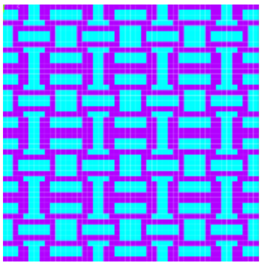

(b) ν_{12} = -0,2014
ν_{21} = -0,2209

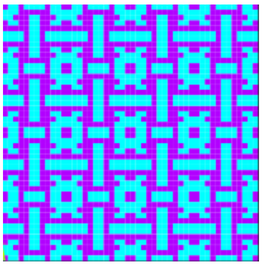

(c) ν_{12} = -0,1282
ν_{21} = -0,3379

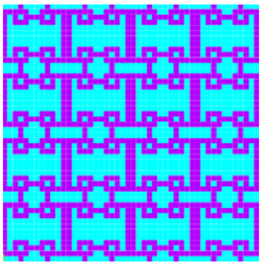

(d) ν_{12} = -0,1754
ν_{21} = -0,0767

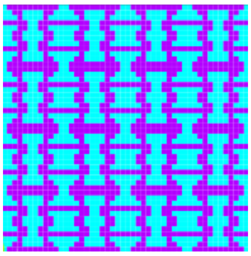

(e) ν_{12} = -0,0155
ν_{21} = -0,0376

Fig. 4-6 The top 5 solutions determined by Bayesian optimization in the latent space of VAE for the 6x6 model

It can be observed that the minimum values obtained using Bayesian optimization in the latent space of the VAE are not lower than those obtained using the greedy algorithm and the CNN model. The initial model used manages to determine structures with lower values of the Poisson coefficient. However, it turns out that Bayesian optimization can also determine auxetic structures.

In addition to optimization in latent space, a trained VAE model can also be used for its generative properties. For example, it can identify families of solutions that have similar characteristics and can be tested for similar properties. Another way to use the generative properties of VAE is to perform interpolation in latent space between two known solutions. Since the latent space is well organized, neighboring solutions have similar characteristics, which is why it is possible to interpolate between two latent vectors, and the results show how to transition from one solution to another by navigating through the solution space. An example of this is shown in Fig. 4-7, where the structures for each interpolation step (a) and the variation of Poisson's coefficients (in the X direction in blue and in the Y direction in orange) corresponding to each configuration in the interpolation space (b) can be seen. The user can use this generative property to determine new solutions that have combined properties. For example, if we know an auxetic structure and a structure with a high transverse elastic modulus, by interpolating between the two, we can determine structures that combine the two properties mentioned.

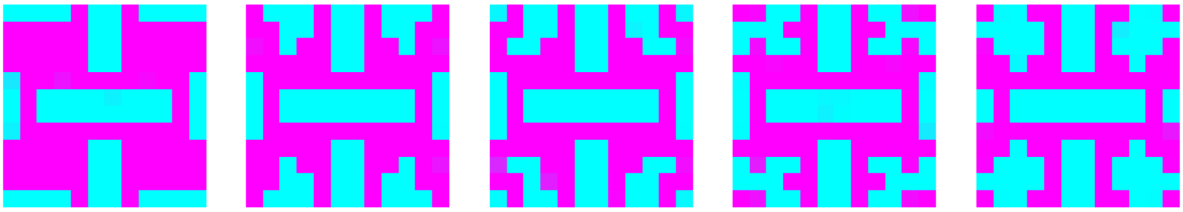

(a)

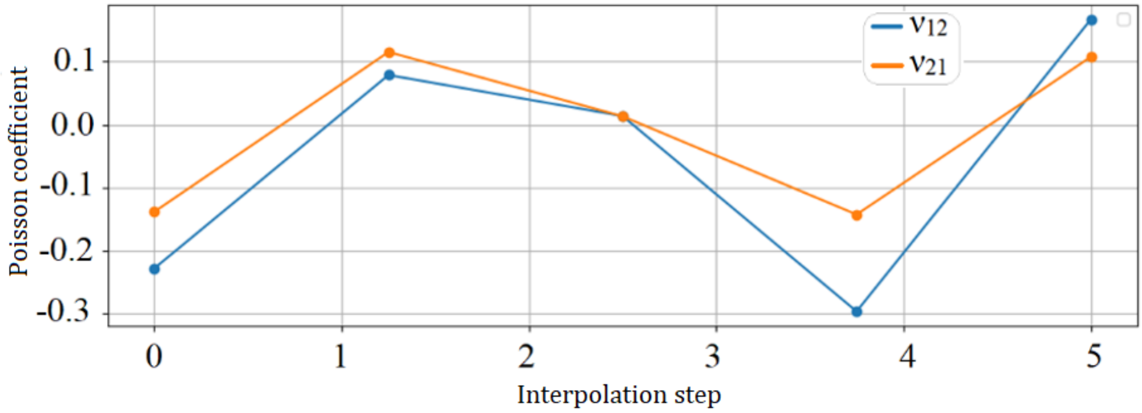

(b)

Fig. 4-7 Interpolation in the latent space between two solutions: (a) configurations obtained in the interpolation steps; (b) variation of Poisson's coefficients for the interpolation steps;

This chapter presents models for solving optimization problems based on artificial intelligence techniques for composite materials with representative volume elements aimed at identifying metamaterials with auxetic behavior. The methodology combines direct search techniques with advanced learning models in order to efficiently determine optimal solutions.

The application of CNN for predicting the mechanical properties of representative volumes has proven to be very effective. By training the network with a dataset consisting of representative volume configurations and Poisson's ratio values representing only 0.006% of the entire solution space, it was able to accurately estimate the mechanical properties of the configurations. The low prediction error of the convolutional neural network highlights the potential of machine learning models in addressing challenges related to computationally expensive simulations.

The optimal solution determined by the greedy algorithm combined with the trained convolutional neural network bears a high resemblance to the cells known in the literature as tetra-anti-chiral. This similarity demonstrates the validity and ability of the optimization model to successfully navigate the solution space. At the same time, the emergence of such a structure highlights the fact that the convolutional neural network model has "learned" and effectively uses the mechanical principles underlying auxetic behavior. The emergence of the tetra-anti-chiral cell-like solution indicates that these solutions are not only theoretically sound, but also arise naturally from data-driven optimization processes, further validating their relevance in the field of metamaterials. Research on the use of CNN+*greedy* for optimizing such structures was published in [17].

CHAPTER 5 – EXPERIMENTAL RESEARCH ON OPTIMIZED PERIODIC COMPOSITE AUXETIC STRUCTURES

Auxetic structures, characterized by a negative Poisson's ratio, have the unusual property of expanding laterally when stretched and contracting when compressed. This behavior results in advantageous mechanical properties, such as high energy absorption, increased shear strength, and superior impact performance, making them attractive for use in protective equipment [18], biomedical implants [19], aerospace components [20], and mechanical metamaterials [21].

The purpose of this chapter is to experimentally verify whether the previously determined auxetic configurations, optimized using a CNN-greedy optimization framework and fabricated by dual-material printing, indeed exhibit auxetic behavior. The tested configurations are repetitive structures with representative volumes similar to anti-chiral tetra geometries composed of a hard material (Ultimaker PETG) and a soft elastomer (BASF TPU85), the distribution of materials being determined by the optimization algorithm.

In the first stage of the experimental study, the mechanical properties of the base materials were determined. PETG test specimens manufactured in accordance with ASTM D638 were tested using an INSTRON universal testing machine and an extensometer that provided accurate measurements of strain. This allowed the determination of the elastic modulus and maximum tensile stress. The experimental results confirmed the mechanical properties defined in the material's technical data sheets with errors of less than 3%. TPU85, being a highly deformable elastomer, was tested using a Zwick testing machine, and the strain data was captured by DIC as the clip-on extensometer could not be mounted on the test specimens. For the elastic modulus of the TPU85 material, an error of 10% was obtained, but for the tensile strength, the error presented is 250% because the conventional curve was used instead of the actual curve of the material. For both materials, the Poisson's ratio was evaluated by DIC using three different methods (1) analysis of the deformation along a central vertical line compared to three horizontal lines in the analysis domain, (2) averaging of specific deformations over the entire analysis region, and (3) tracking the displacement of the corner points of the rectangular DIC analysis domain. All three methods indicated approximately the same Poisson's ratio values for the specimens made homogeneously from the base materials.

For auxetic configurations, DIC was the main tool used (Fig. 5-1) to measure strain fields and calculate Poisson's ratio.

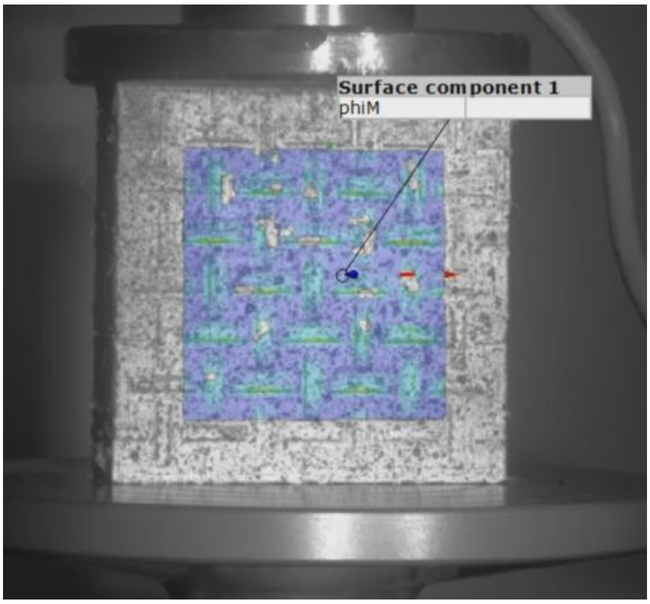

Fig. 5-1 Image during DIC analysis - auxetic configuration

Of the methods used on the base material samples, only method 3 showed promising results, the other two methods being difficult to implement and producing high error rates. In this regard, a methodology presented in the literature was applied to determine Poisson's ratio using 12 different variants. These approaches allowed both cross-validation and increased confidence in the measured values, despite the high complexity of analyzing repetitive structures in multiple materials.

Two optimized configurations (shown in Fig. 5-2) were selected for testing: configuration A with 55% hard materials and configuration B with 41%. Four specimens were made for each configuration. The same formulas were applied to determine Poisson's ratio, and the average results were compared with the results obtained through numerical simulations under the assumption of a plane stress state and a plane strain state, respectively. The results were convincing: three of the four samples for each configuration showed a negative Poisson's ratio, confirming the auxetic nature of these structures. Configuration A consistently showed strong agreement with the simulated results, presenting a range of negative Poisson's ratios between -0.25 and -0.74. Configuration B, although showing auxetic tendencies, showed less consistency, with Poisson ratios between -0.07 and -0.24 and a greater deviation from the results obtained by numerical simulation.

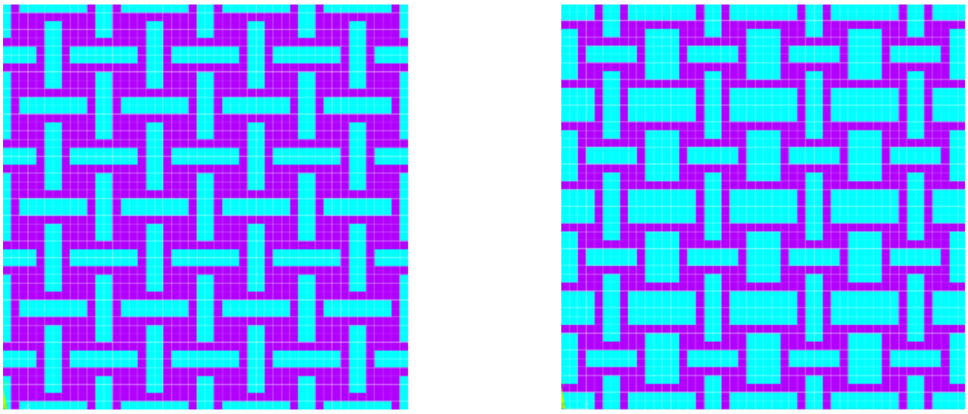

(A) (B)

Fig. 5-2 Auxetic structures optimized using CNN and the greedy algorithm; (A) 55.56% hard material; (B) 41.66% hard material

The larger errors in configuration B can be attributed to several factors. First, the higher percentage of soft material likely made the structure more sensitive to inconsistencies in the printing process. TPU85 and PETG have significantly different thermal properties, and the fused deposition manufacturing process introduces potential challenges at the material interface. Low adhesion between the two materials was observed in a tensile test that was considered a failure. At the same time, it was observed that some samples exhibited different colors of the base materials, which may indicate mixing of the two materials during the printing process and the introduction of errors through additional stiffening of the soft parts. In addition, the printing equipment did not have the necessary precision to ensure high repeatability, especially for printing multiple materials.

From a DIC analysis perspective, auxetic configurations presented several challenges. The process of painting the specimens was complicated by differences in level between areas with different materials, as the surface of the specimen was not perfectly flat. Due to large local deformations of the soft material areas, many tracking points were lost during the test, making it difficult to reconstruct the deformation field in some regions. However, by carefully selecting reference areas and analysis methods, significant results were obtained.

In conclusion, experimental research supports the hypothesis that these repetitive two-material structure configurations optimized by the CNN-greedy algorithm may indeed exhibit auxetic behavior. The results validated the predicted performance of configuration A with high accuracy and provided partial confirmation for configuration B. This provides a promising basis for further exploration of design strategies for mechanical metamaterials.

However, the study also highlights several limitations. Dependence on precise material printing and interfacial adhesion remains a major obstacle to the repeatable and high-quality fabrication of multi-material auxetic structures. In addition, although DIC analysis has shown promising results, it requires initial processing of the surfaces of test specimens consisting of two materials with an auxetic configuration.

CHAPTER 6 – METHODOLOGY FOR USING OPTIMIZATION PROCEDURES

The methodology for using optimization procedures presented in this chapter outlines a systematic workflow that guides the entire process, from defining the problem to validating the solution. The methodology begins with a clear definition of the optimization problem, addressing what is being optimized, under what constraints, and for what purpose. By defining the boundary conditions, load cases, and mathematical formulation of the objective function, this step ensures that the optimization process is well defined both theoretically and in terms of practical relevance. The methodology for applying the optimization framework is schematically represented in Fig. 6-1.

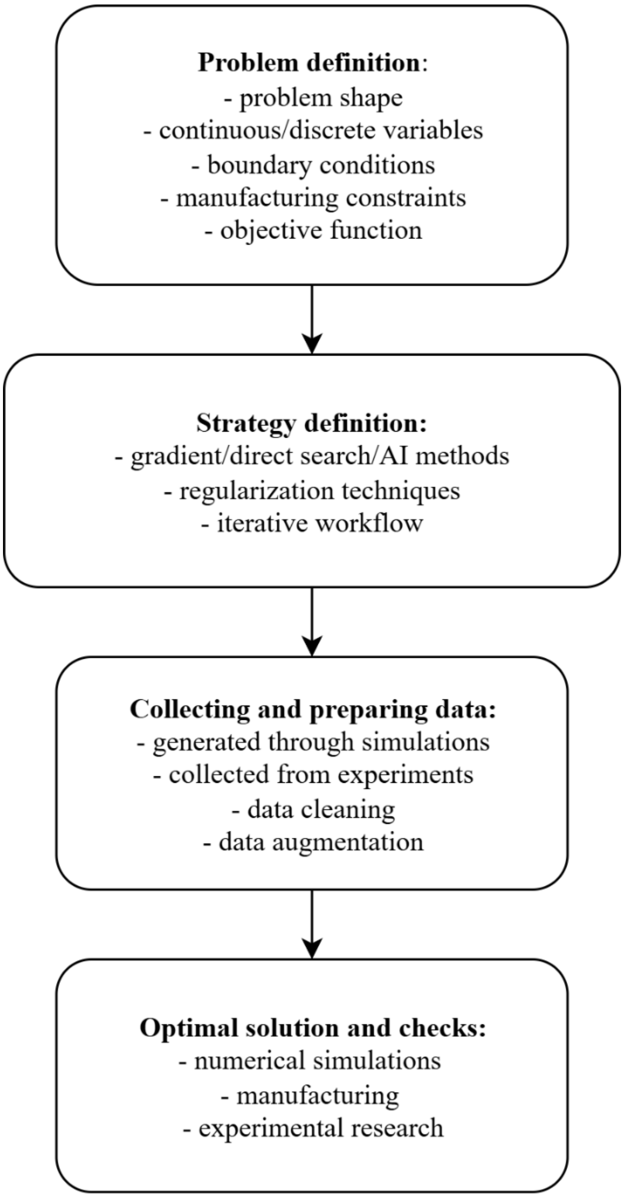

Fig. 6-1 Outline of the methodology for using optimization procedures

The optimization strategy defines how the problem is approached and solved, selecting appropriate algorithms from gradient-based techniques, direct search methods, or AI-based approaches. The next step highlights the importance of data collection and preparation, especially when using ML models, ensuring that the input datasets are both representative and structured to capture the complexity of the problem. Once the data is available, the process of obtaining the optimal solution can be implemented, during which convergence and computational efficiency are monitored.

The final stage of verification and validation of the solution highlights that optimization does not end with a numerical result. Verification through simulations, experimental tests, sensitivity analyses, and comparisons with the literature ensures that the proposed solution is robust, feasible, and aligned with practical applications. At the same time, recognition of limitations—such as the possibility of local optima or manufacturing constraints—keeps the process grounded in reality. Taken together, these workflow steps provide a coherent methodology for structural optimization, maintaining a balance between theoretical formulation and practical applicability, establishing a versatile framework that can be adapted to various problems.

CHAPTER 7 – FINAL CONCLUSIONS

7.1 General conclusions

The doctoral thesis presents a methodology for optimizing periodic composite structures using direct search methods and AI-based methods. The optimization framework is versatile and can be modified and applied to other types of structural optimization problems. Finally, experimental research is conducted on some auxetic composite structures optimized with the previously developed framework, as a case study. Based on the above, the following general conclusions can be drawn:

- The PyAnsys package was used to implement the algorithms, which proved to be highly versatile. It creates an easy development framework between the Python programming language, which allows the creation of calculation routines and mathematical algorithms for optimization, and the ANSYS program, which allows finite element analysis of the solutions found by the optimization algorithms. The PyAnsys package allows closed-loop work without the need to use multiple programs at the same time.
- In defining the optimization problem, a number of important points were analyzed, among which we can mention:
  - The mathematical formulation of the objective function is of particular importance to the optimization process. First, the objective function must ensure that the ultimate goal of the optimization process is translated into mathematical terms. Second, the mathematical formulation must be simple and clear so that it can be easily determined in the iterative optimization process.
  - For periodic structures, it is recommended that the analysis be performed on a representative volume and that periodic conditions be used. In the case of the problem defined in the thesis, due to the double symmetry conditions of the representative volume, the analysis could be performed on a cell sphere, considerably reducing the calculation time for a single solution.
  - Regularization techniques can have a decisive influence on the optimal solution. A convergence study was conducted on composite structures, where it was demonstrated that elements arranged in a chessboard pattern introduce large calculation errors. It was shown that for an increase in the mesh size in a material domain of the representative cell, the optimal solution differs for the same formulation of the objective function. The implementation of regularization techniques such as specialized functions for eliminating solutions with chessboard pattern was subsequently successfully implemented, demonstrating their necessity.
  - The use of discrete or continuous optimization variables changes the nature of the process. In the problem described in the doctoral thesis, discrete variables were used, and it was shown that for small sizes of the representative volume, the optimum can be determined using a brute force approach. At the same time, it was shown that the total number of solutions increases considerably for a relatively small increase in the size of the representative volume from 4x4 to 6x6. Hardware limitations mean that the brute force approach can only be used for limited problems. In the case of problems with continuous optimization variables, the total number of solutions is infinite, and such an approach cannot be used.

- A comparative analysis of four direct search algorithms was performed to determine the previously defined structures with maximized elastic moduli along the two orthogonal directions, from which the following conclusions were drawn:
    - The greedy algorithm is easy to implement and offers promising results. At the same time, the optimal solution determined by it depends on the starting point. For the 4x4 configuration, it had a success rate of 86% with an average of 227.2 evaluations of the objective function.
    - The SA algorithm, although it performed well in other studies, did not stand out in the ranking. As defined, the algorithm is a chain of greedy algorithms designed to eliminate the disadvantage of dependence on the starting point. For the 4x4 configuration, it had a success rate of 100% but with an average of 1,868.16 objective function evaluations, i.e., a computational effort 8 times greater than that of the greedy algorithm.
    - From the evolutionary algorithms category, GA and PSO were applied to the 4x4 configuration, and the results were promising. GA showed a 100% success rate with an average objective function evaluation of 578, and PSO showed a 100% success rate with an average objective function evaluation of 179.5.
    - After scaling the problem to the 6x6 configuration, GA proved to be ineffective for solving this type of problem with the highest computational effort required and the lowest value obtained for the objective function.
    - Among the algorithms tested on the 4x4 configuration, PSO showed the best balance between computational effort and the average objective function value obtained for the 6x6 configuration.
    - A hybrid PSO+greedy approach was implemented, offering the best performance in terms of computational effort and objective function value. The hybrid approach achieved an average objective function value of 3.7511, an improvement of approximately 4% over the PSO algorithm, for an average number of solutions evaluated equal to 4,555.2, i.e., an improvement of approximately 20% in computational effort.
- In order to implement AI-based methods for solving structural optimization problems, a database is required. The main considerations to be taken into account for the construction of the database were presented, from consistency in data storage and data normalization, whether we are talking about data generation or data collection. Data augmentation processes, which multiply the training database, were of particular importance in facilitating the training process.
- To solve a problem of optimizing the distribution of a composite material in order to obtain configurations with negative values of Poisson's ratio, two AI-based methods were tested: one method using a convolutional neural network to predict the Poisson's ratio of a given configuration together with a greedy algorithm to determine the optimum, and one method using a variational autoencoder. The following conclusions were drawn from the construction of the two methods:
    - For CNN, an analysis of the number of layers and their structure was performed. For both the 4x4 and 6x6 configurations, 9-layer networks were developed with max pooling and convolution layers. The construction proved to be robust for both configurations and allowed transfer learning from the 4x4 configuration to the 8x8 configuration. It was found that augmenting the training dataset significantly

reduced the network validation error at the end of the training stage, and transfer learning influenced the initial loss value, showing the potential to reduce the number of training epochs required.

  - For VAE, the encoder construction involved an input layer, three convolution layers with 16, 32, and 64 filters, respectively, followed by a flattening and densification layer. The decoder construction is similar to that of the encoder, only with the layers reversed. An analysis was performed on the influence of the number of latent variables on the reconstruction loss, which resulted in an optimum of 12 variables. At the same time, it was demonstrated that the increased number of latent variables also increased the KL loss. In this regard, a training strategy was approached with the application of the β weight in the evaluation of the KL loss, which led to a significant improvement in the total loss at the end of the training process.

- The performance of AI-based methods was verified using various metrics:
  - For CNN, the validation error value in the 4x4 configuration reached 0.00008 for training with 90% of the total solutions, and in the 6x6 configuration it reached 0.004 for training with 0.0003% of the total solutions. The value predicted by the network was compared with the actual value obtained by finite element analysis for Poisson's ratio in both configurations, 4x4 and 6x6, respectively, where high accuracy was observed in the prediction of Poisson's ratio for a given material configuration.
  - For VAE, the pair diagram of latent variables showed a normal distribution for all 12 variables, indicating that training was performed in accordance with the requirements of a variational autoencoder. Dimensionality reduction techniques were applied to the latent variable space so that five groups of solutions with similarities in construction could be identified. Although the total loss value remained around 30, it was comparable to other models developed in the literature.
- The trained 6x6 CNN network enabled the construction of an optimization framework together with a greedy algorithm that provided a variety of solutions with negative Poisson coefficient values. The optimal solution discovered recorded a Poisson coefficient value of -0.4543 for both orthogonal directions. The CNN-greedy optimization framework proved to be very efficient, combining the predictive power of the Poisson coefficient with minimal CNN network computation effort, along with the greedy algorithm's ability to easily navigate the solution space to determine the optimum.
- The trained variational autoencoder was used together with a Bayesian optimization framework in the latent space. This framework did not find solutions as good as those found by the CNN-greedy framework, with the minimum Poisson coefficient recorded being -0.3379 for one of the directions. Even though the solutions obtained did not have the same performance, VAE showed generative abilities that can be exploited in other conditions, such as classifying solutions into families or interpolating in the latent space between two solutions to discover configurations with similarities in construction between the two.
- Experimental research was conducted on a case study of configurations obtained by optimizing auxetic composite structures, from which the following conclusions were drawn:

- In the first experimental stage, the mechanical properties of the base materials were determined. The PETG specimens were tested for tensile strength (ASTM D638) on an INSTRON machine with an extensometer, obtaining values for the elastic modulus and tensile strength within 3% of the values in the technical data sheet. The TPU85 material, also tested for tensile strength on a Zwick machine with DIC due to its high deformability, showed an error of 10% in the value obtained for the elastic modulus and a higher error of 250% for the tensile strength value, apparently caused by the use of the conventional curve instead of the actual one. Poisson's ratio for both materials was evaluated using DIC with three methods, all of which provided consistent results.
- For auxetic configurations, tensile tests showed that the adhesive force between these two materials is very low, which led to premature delamination during the tensile test. The results were inconsistent for the tensile tests, and a review of the literature on interfacial adhesion forces of plastics manufactured using FDM technology showed that the problem is complex and difficult to solve.
- DIC was the main tool for measuring strain and evaluating Poisson's ratio for compression tests performed on optimized auxetic configurations. Of the methods used, only tracking the deformation of the corners of a selected domain proved reliable, while the others showed large errors. A methodology from the literature was adopted, applying 12 calculation variants to allow cross-validation and increase confidence, despite the complexity of the analysis of periodic multi-material structures.
- Two optimized configurations were tested: configuration A (55% rigid material) and configuration B (41% rigid material). Four samples from each configuration were analyzed, and the average values obtained for Poisson's ratio were compared with numerical simulations under the assumption of a plane stress and a plane strain, respectively. The results confirmed auxetic behavior in three out of four samples for each case. Configuration A closely aligned with the simulations (–0.25 to –0.74), while configuration B showed a greater deviation (–0.07 to –0.24).
- The larger errors in configuration B were attributed to the higher soft material content, which makes it more sensitive to print quality. The problems were caused by poor PETG-TPU adhesion, interfacial defects, and observed evidence of partial mixing of materials, which stiffened the soft regions. Printing accuracy was also insufficient for reliable reproducibility of multiple materials, further contributing to the variability obtained.
- DIC analysis of auxetic samples faced challenges such as uneven surfaces between hard and soft phases and data loss in highly deformable TPU regions. However, by carefully defining reference areas and methods, significant deformation fields were obtained, validating the feasibility of using DIC for such complex structures.
- Experiments confirmed that these configurations optimized using the CNN-greedy framework can exhibit auxetic behavior. Configuration A substantially validated the predictions, while configuration B provided partial confirmation. However, limitations were also observed, including difficulties in accurate multi-material printing, poor interfacial adhesion, and the need for careful specimen preparation in DIC analysis.

7.2 Personal contributions

A series of personal contributions have been made to methods for optimizing special configuration structures as well as experimental methods such as:

- Creating a working framework with the PyAnsys package for developing optimization algorithms in the Python programming language while calling the ANSYS finite element analysis program (Subchapter 3.3.1).
- Performing a comparative analysis of the performance in solving structural optimization problems of four direct search algorithms: greedy, SA, GA, and PSO (Subchapter 3.3.2.).
- Developing optimization algorithms in such way to allow easy modification of parameters for scaling to larger problem sizes. (Subchapter 3.3.3).
- Developing and training a convolutional neural network that predicts with low error the material properties of special configuration structures (Subchapters 4.3.2., 4.3.3., and 4.3.4.).
- Developing and training a variational autoencoder that encodes the solution space with 12 latent variables with a normal distribution and allows their reconstruction with high accuracy (Subchapters 4.3.2., 4.3.3., and 4.3.4.).
- Creating a CNN-greedy optimization framework that uses the predictive power of the convolutional neural network and the ability of the greedy algorithm to navigate the solution space in order to determine the optimal solutions for large-scale problems (Subchapter 4.4.).
- Adjusting the parameters of FDM printing equipment to achieve efficient multi-material printing (Subchapter 5.2.)
- Development, verification, and validation of three methods for determining Poisson's ratio for homogeneous specimens using DIC digital image correlation equipment (Subchapter 5.3.2.).
- Development of a procedure for determining Poisson's ratio using DIC for periodic composite structures with the help of control lines passing through predefined points in the structure, averaging the specific deformations over the entire length of the control lines (Subchapter 5.4.2.).
- Synthesizing and structuring the steps of the procedure for optimizing special configuration structures into a methodology for use, with a view to easy application by other users for various problems (Chapter 6).

7.3 Future research

- Extending the optimization framework to enable the optimization of repetitive three-dimensional structures with different objective functions in order to expand the library of architectured material structures.
- Broadening the optimization framework to include three or more materials, which could open up much richer design possibilities. A rigid phase, a highly deformable phase for energy absorption, and an intermediate phase for adjusting local stiffness or improving the adhesive force between materials could be combined.

- Implementing other artificial intelligence methods for structure optimization. Exploiting generative methods to discover other structures with novel properties and geometries.
- Developing an integrated application that facilitates the user in defining the optimization problem of special configuration structures, setting the objective function, choosing the optimization algorithm, generating the training data set in the case of AI-based approaches, training, and searching for optimal solutions.
- Refining multi-material additive manufacturing processes to improve repeatability and interfacial adhesion forces between materials. Verifying other hybrid manufacturing methods (printing one phase of material and casting or injecting the other phase) of multi-material structures with complex geometry.
- Improving procedures for verifying the mechanical properties of optimized structures using other complex systems such as X-ray scanning or computed tomography to verify the behavior of structures within the working volume.

BIBLIOGRAPHY

[1] C. Pan, Y. Han, and J. Lu, "Design and Optimization of Lattice Structures: A Review," *Appl. Sci.*, vol. 10, no. 18, p. 6374, 2020, doi: 10.3390/app10186374.

[2] L. Zheng, S. Kumar, and D. M. Kochmann, "Data-driven topology optimization of spinodoid metamaterials with seamlessly tunable anisotropy," *Comput. Methods Appl. Mech. Eng.*, vol. 383, p. 113894, 2021, doi: 10.1016/j.cma.2021.113894.

[3] B. Zhu, X. Zhang, H. Zhang, J. Liang, H. Zang, H. Li and R. Wang., "Design of compliant mechanisms using continuum topology optimization: A review," *Mech. Mach. Theory*, vol. 143, 103622, 2020, doi: 10.1016/j.mechmachtheory.2019.103622.

[4] R. M. Gorguluarslan and Y. Yamaner, "Self-supporting robust lattice optimization for material extrusion additive manufacturing," *Compos. Struct.*, vol. 371, no. April, p. 119470, 2025, doi: 10.1016/j.compstruct.2025.119470.

[5] H. Yan, W. T. Wu, Z. Zhao, and F. Feng, "Review and comparison of turbulent convective heat transfer in state-of-the-art 3D truss periodic cellular structures," *Appl. Therm. Eng.*, vol. 235, no. August, p. 121450, 2023, doi: 10.1016/j.applthermaleng.2023.121450.

[6] S. Song, C. Xiong, and J. Yin, "Mechanical performance of reinforced hybrid periodic-multicell thin-walled structures in sandwich applications: A review," *Thin-Walled Struct.*, vol. 208, no. December 2024, p. 112832, 2025, doi: 10.1016/j.tws.2024.112832.

[7] S. Kumar, S. Tan, L. Zheng, and D. M. Kochmann, "Inverse-designed spinodoid metamaterials," *npj Comput. Mater.*, vol. 6, no. 1, pp. 1–10, 2020, doi: 10.1038/s41524-020-0341-6.

[8] M. P. Bendsøe and O. Sigmund, *Topology Optimization. Theory, Methods, and Applications*. Springer-Verlag Berlin Heidelberg, 2004.

[9] D. W. Abueidda, M. Elhebeary, C. S. (Andrew) Shiang, S. Pang, R. K. Abu Al-Rub, and I. M. Jasiuk, "Mechanical properties of 3D printed polymeric Gyroid cellular structures: Experimental and finite element study," *Mater. Des.*, vol. 165, p. 107597, 2019, doi: 10.1016/j.matdes.2019.107597.

[10] "ISO/ASTM 52900:2021 Additive manufacturing — General principles — Fundamentals and vocabulary," 2021.

[11] B. Hassani and E. Hinton, *Homogenization and Structural Topology Optimization.*, Springer London, 1999.

[12] G. X. Gu, L. Dimas, Z. Qin, and M. J. Buehler, "Optimization of Composite Fracture Properties: Method, Validation, and Applications," *J. Appl. Mech. Trans. ASME*, vol. 83, no. 7, pp. 1–7, 2016, doi: 10.1115/1.4033381.

[13] I. C. Coropețchi, D. M. Constantinescu, A. Vasile, Șt Sorohan, and D. A. Apostol, "Comparative analysis of direct search methods for material design optimization," *Proc. Inst. Mech. Eng. Part L J. Mater. Des. Appl.*, vol. 239, no. 4, pp. 642–660, 2025, doi: 10.1177/14644207241294056.

[14] I. C. Coropețchi, D. M. Constantinescu, A. Vasile, A. I. Indreș, Ștefan Sorohan, and D. A. Apostol, "Direct search methods for determining new designs of auxetic materials," *J. Theor. Appl. Mech.*, vol. 63, no. 3, pp. 479–489, 2024, doi: 10.15632/jtam-pl/200711.

[15] S. Teraiya, S. Vyavahare, and S. Kumar, “Numerical and Experimental Investigation on Effect of Design Factors on Shear Properties of Additively Manufactured Tetra-Anti-Chiral Cellular Metamaterial,” *Int. J. Mod. Manuf. Technol.*, vol. 14, no. 1, pp. 104–112, 2022, doi: 10.54684/ijmmt.2022.14.1.104.

[16] H. I. On, L. Jeong, M. Jung, D. J. Kang, J. H. Park, and H. J. Lee, “Optimal design of microwave absorber using novel variational autoencoder from a latent space search strategy,” *Mater. Des.*, vol. 212, 2021, doi: 10.1016/j.matdes.2021.110266.

[17] I. C. Coropețchi, D. M. Constantinescu, A. Vasile, A. I. Indreș, and Ștefan Sorohan, “Design of Novel Auxetic Bi-Materials Using Convolutional Neural Networks,” *Materials*, vol. 18, no. 8, 1772, 2025, doi: 10.3390/ma18081772.

[18] M. I. Khan, M. Umair, and Y. Nawab, „Use of auxetic material for impact/ballistic applications”, *Composite Solutions for Ballistics,* pp. 199-228, Elsevier, https://doi.org/10.1016/B978-0-12-821984-3.00012-7, 2021.

[19] S. Rose, D. Siu, J. Zhu, and R. Roufail, “Auxetics in Biomedical Applications: A Review,” *J. Miner. Mater. Charact. Eng.*, vol. 11, no. 02, pp. 27–35, 2023, doi: 10.4236/jmmce.2023.112003.

[20] Z. Wang, H. Zulifqar, and H. Hu, “7 - Auxetic composites in aerospace engineering,” in *Advanced Composite Materials for Aerospace Engineering Processing, Properties and Applications*, S. Rana and R. Fangueiro, Eds. Woodhead Publishing, 2016, pp. 213–240.

[21] V. Siniauskaya, H. Wang, Y. Liu, Y. Chen, M. Zhuravkov, and Y. Lyu, “A review on the auxetic mechanical metamaterials and their applications in the field of applied engineering,” *Front. Mater.*, vol. 11, no. August, pp. 1–14, 2024, doi: 10.3389/fmats.2024.1453905.